



# Hydrogels from Amorphous Calcium Carbonate and Polyacrylic Acid: Bio-Inspired Materials for “Mineral Plastics”

Shengtong Sun, Li-Bo Mao, Zhouyue Lei, Shu-Hong Yu, and Helmut Cölfen\*

**Abstract:** Given increasing environmental issues due to the large usage of non-biodegradable plastics based on petroleum, new plastic materials, which are economic, environmentally friendly, and recyclable are in high demand. One feasible strategy is the bio-inspired synthesis of mineral-based hybrid materials. Herein we report a facile route for an amorphous  $\text{CaCO}_3$  (ACC)-based hydrogel consisting of very small ACC nanoparticles physically cross-linked by poly(acrylic acid). The hydrogel is shapeable, stretchable, and self-healable. Upon drying, the hydrogel forms free-standing, rigid, and transparent objects with remarkable mechanical performance. By swelling in water, the material can completely recover the initial hydrogel state. As a matrix, thermochromism can also be easily introduced. The present hybrid hydrogel may represent a new class of plastic materials, the “mineral plastics”.

**L**iving organisms exploit minerals, especially calcium carbonate and calcium phosphate, to build a variety of inorganic–organic hybrid materials for various specific functions, such as protection, mechanical support, photonics, or navigation.<sup>[1–3]</sup> Their perfect control over the composition, morphology, and hierarchical structures of biominerals has inspired material scientists to design new artificial materials with remarkable properties.<sup>[4–6]</sup> Often, mineralization takes place in gel-like matrices, which are three-dimensional macromolecular assemblies of proteins, polysaccharides, and/or glycoproteins.<sup>[7]</sup> Once formed, biominerals, such as bone, teeth, and nacre, have definite shapes owing to the extrusion of the

organic matrix and/or the irreversible crystallization of amorphous precursors.<sup>[8,9]</sup> Calcium-based biominerals typically contain around 0.1–1 wt% acidic proteins, such as the Asp-rich proteins,<sup>[10]</sup> and acidic macromolecules are seen as the control molecules for nucleation and crystallization. Therefore, a transient “polymer-induced liquid precursor” (PILP) phase induced with ppm amounts of a polyacid can play an important role during crystallization.<sup>[11–14]</sup> If the transient liquid or amorphous mineral phase can be long-term stabilized by polymer additives, then the idea of producing amorphous mineral-based supramolecular hydrogels that may be shapeable and solidify reversibly is promising.

Biominerals with a hybrid structure of organic matrices and amorphous minerals can be found in organisms, such as cystoliths<sup>[15]</sup> and shrimp shells.<sup>[16,17]</sup> For instance, a transparent exoskeleton of living *Pandalus borealis*<sup>[16]</sup> or *Marsupenaeus japonicus*<sup>[17]</sup> consists of mainly chitin, proteins, and amorphous calcium carbonate (ACC). Synthetically, Kato et al. fabricated transparent hybrid films comprising ACC and polyacrylic acid (PAA) with nanosegregated structures,<sup>[18]</sup> which can be further reinforced by nanocellulose networks.<sup>[17]</sup> A transparent cellulose–ACC film<sup>[19]</sup> and cellulose–amorphous  $\text{CaSO}_4$  film<sup>[20]</sup> were also reported. Nevertheless, none of these materials was able to form a hydrogel before drying or after re-immersing in water. Incorporating mineral particles into a hydrogel matrix or in situ growing crystalline minerals in hydrogels produces nanocomposite hydrogels with good mechanical performance or novel structures, but their gelling property largely relies on the polymer matrix itself.<sup>[21–25]</sup> For example, Schmidt et al. prepared highly extensible and elastomeric nanocomposite hydrogels by mixing poly(ethylene glycol) and hydroxyapatite nanoparticles; however, due to the chemical cross-linking of the poly(ethylene glycol) network, the hydrogel is not shapeable and self-healable.<sup>[24]</sup> A macroscopic ACC-based hybrid gel-like disk was obtained by Xia et al. by mineralizing  $\text{CaCO}_3$  within a PNIPAM microgel dispersion, which is very weak and easily disassembled upon vigorous shaking and rinsing, and cannot even be regarded as a “hydrogel”.<sup>[26]</sup> Herein, we report a well-defined ACC-based hybrid supramolecular hydrogel by simply mixing  $\text{CaCl}_2$ ,  $\text{Na}_2\text{CO}_3$ , and PAA in water. The resulting hydrogel is shapeable and stretchable with novel self-healing and shear-thinning characteristics, and can be recovered by swelling the dried transparent film. Thermochromism can also be introduced into the hydrogel matrix resulting in colorimetric hybrid materials.

The ACC–PAA hybrid hydrogel was synthesized by slowly adding 0.1M  $\text{Na}_2\text{CO}_3$  into a mixed solution of 0.1M  $\text{CaCl}_2$  and 0.1M PAA ( $M_w \approx 100\,000 \text{ g mol}^{-1}$ ) with vigorous stirring (Figure 1a). A white sticky precipitate gradually

[\*] Dr. S. T. Sun, Prof. Dr. H. Cölfen  
Physical Chemistry  
University of Konstanz  
Universitätsstrasse 10, 78457 Konstanz (Germany)  
E-mail: helmut.coelfen@uni-konstanz.de

L. B. Mao, Prof. Dr. S. H. Yu  
Division of Nanomaterials and Chemistry, Hefei National Laboratory for Physical Sciences at Microscale, Department of Chemistry, University of Science and Technology of China  
Hefei, Anhui 230026 (P.R. China)

Z. Y. Lei  
State Key Laboratory of Molecular Engineering of Polymers, Department of Macromolecular Science, Laboratory for Advanced Materials, Fudan University  
Shanghai 200433 (P.R. China)

Dr. S. T. Sun  
Current address: School of Chemical Engineering, State Key Laboratory of Chemical Engineering, Shanghai Key Laboratory of Multiphase Materials Chemical Engineering, East China University of Science and Technology  
130 Meilong Road, Shanghai 200237 (P.R. China)

Supporting information for this article can be found under: <http://dx.doi.org/10.1002/anie.201602849>.

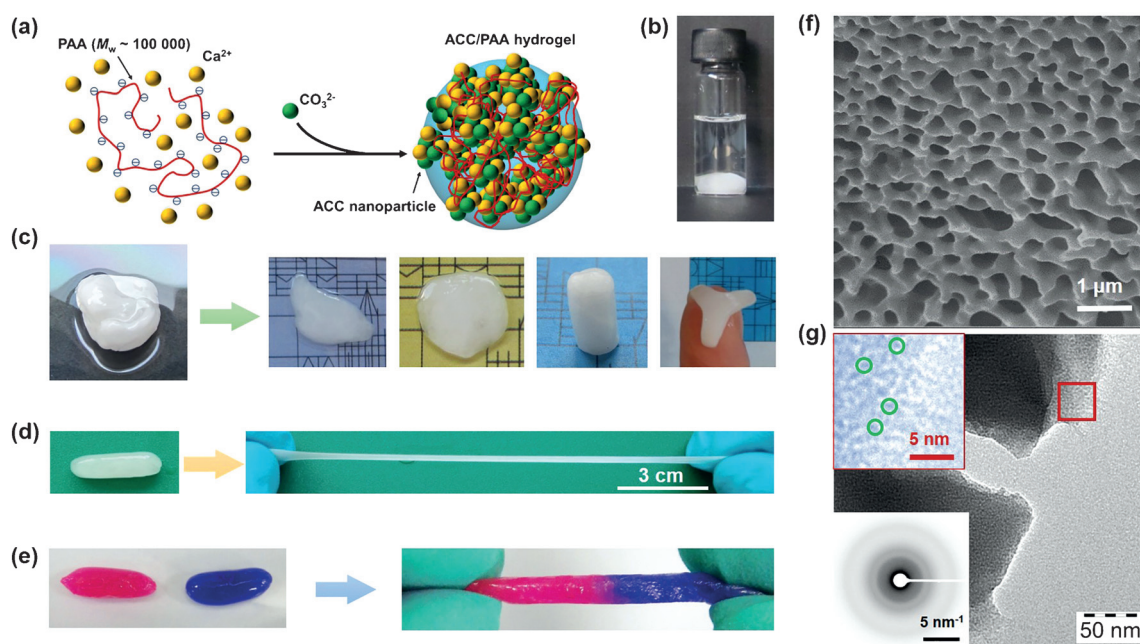


**Figure 1.** a) Schematic synthesis of the ACC/PAA supramolecular hydrogel. b) ACC/PAA hydrogel is stable in water. c) ACC/PAA hydrogel is plastic, which can be made in different shapes. d) ACC/PAA hydrogel is stretchable. e) Self-adhesion of ACC/PAA hydrogel. Dye molecules (rhodamine B and methylene blue) were introduced to produce the colors. f) SEM image of the freeze-dried ACC/PAA hydrogel. g) TEM images of ACC/PAA dry gel. The insets are the corresponding electron diffraction pattern and an enlarged view of the area highlighted by the red square illustrating the presence of very small ACC nanoparticles (highlighted by green circles).

formed around the stirring bar, resulting in a turbid solution containing non-gelling fractions. The obtained hydrogel was thoroughly washed by deionized water until the solution is clear. It should be noted that the molecular weight of PAA is important for the hydrogel formation; too short (ca.  $2000 \text{ g mol}^{-1}$  or ca.  $5100 \text{ g mol}^{-1}$ ) or too long (ca.  $450000 \text{ g mol}^{-1}$ ) PAA chains gave no hydrogels but weak precipitates. When the  $M_w$  of PAA is  $2000 \text{ g mol}^{-1}$ , the precipitate can be redispersed in water, as reported<sup>[17,18,27]</sup> (Supporting Information, Figure S1), while for  $M_w \approx 100000 \text{ g mol}^{-1}$ , the hydrogel cannot be dispersed again (Figure 1b). The reason for the chain-length-dependent gelling ability of PAA is likely the chain-length dependent number of  $\text{Ca}^{2+}$  cross-links, which hinder redispersion beyond a critical value. Furthermore, the concentration of PAA is also key to the hydrogel formation. The minimal concentration of PAA to form a hydrogel is approximately  $0.08 \text{ M}$ ; lower than this, crystalline  $\text{CaCO}_3$  begins to appear.

The resultant hydrogel possesses a few interesting features. For instance, the hydrogel is shapeable, and may be regarded as a “mineral plastic”. The hydrogel is a dough-like material, soft but tough, and can be formed into different shapes, such as films, cylinders, and stars (Figure 1c). The hydrogel is also stretchable. It may be stretched into very long fibers with plastic deformation without any elastic recovery (Figure 1d). Additionally, the hydrogel can self-heal rapidly; within 5 s when linking two parts together (Figure 1e, see Supporting Movies 1 and 2 for the dynamic self-healing process). A control experiment of chemically cross-linked poly(*N,N*-dimethylacrylamide) hydrogels is also presented showing no self-healing properties (Figure S2). A SEM image

of the freeze-dried ACC/PAA hydrogel shows a porous internal structure (Figure 1f), typical for hydrogels.<sup>[28]</sup> Very small ACC nanoparticles ( $1.5\text{--}3 \text{ nm}$ ) can be identified in the TEM image of the dry gel (Figure 1g), indicating that the hydrogel is actually a complex of ACC nanoparticles physically cross-linked by PAA chains via coulomb interactions between  $\text{COO}^-$  and  $\text{Ca}^{2+}$ . Similar particles and their cross-linking can be observed in the TEM image of a freeze-dried sample (Figure S3). Apparently, once formed, the aggregation of ACC nanoparticles for further growth or crystallization is significantly inhibited by the PAA chains. The amorphous nature of  $\text{CaCO}_3$  in the hybrid can also be confirmed by polarized optical microscopic images (Figure S4). An energy dispersive X-ray spectrum (EDS) shows the presence of calcium and the complete removal of sodium salts (Figure S5). The ATR-FTIR spectrum indicates the presence of ACC in the hybrid and the chelation interaction between  $\text{COO}^-$  and  $\text{Ca}^{2+}$  (Figure S6). The solid content of the fully swollen ACC/PAA hydrogel was estimated to be 38–42 wt%. For the dried gel, the molar ratio of different components,  $[\text{CaCO}_3]:[\text{PAA}]:[\text{water}]$ , was calculated to be 39:74:44 by TGA (Figure S7). Interestingly, judging from TGA, ACC/PAA hydrogels prepared at different concentrations of PAA exhibit very similar compositions, indicating that PAA tends to bind a certain amount of ACC nanoparticles.

All the features of the ACC/PAA hydrogel are closely related to its rheological properties. As shown in Figure 2a, the viscoelasticity of the hydrogel varies significantly with the angular frequency, which can be explained by its physically cross-linked nature. The dynamic storage modulus ( $G'$ ) is very

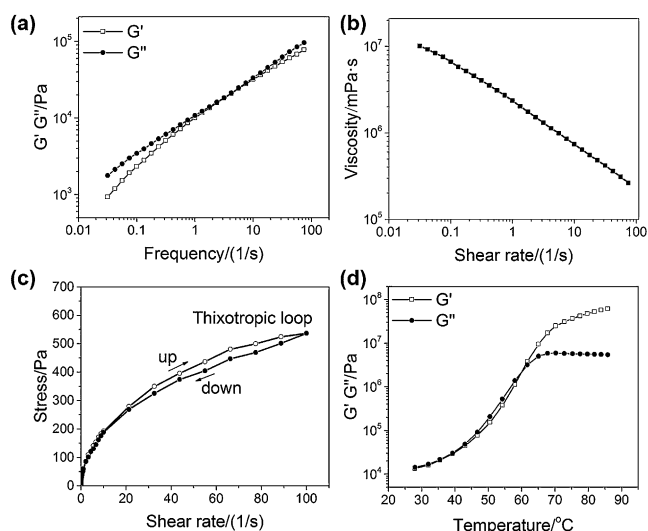


**Figure 2.** Rheological behavior of the ACC/PAA hydrogel. a) Frequency dependencies of the storage ( $G'$ ) and loss ( $G''$ ) moduli. b) Viscosity as a function of shear rate. c) Thixotropic loop measurement. d) Temperature dependencies of the storage ( $G'$ ) and loss ( $G''$ ) moduli.

close to, or only slightly lower than the loss modulus ( $G''$ ), indicating the semi-liquid state of the hydrogel with a slightly dominant role of viscosity. The hydrogel is also tougher, judging from the higher values of  $G'$  and  $G''$  ( $10^3$ – $10^5$  Pa), than normal hydrogels ( $< 1000$  Pa)<sup>[29]</sup> due to the incorporation of large amounts of minerals. As the shear rate increases, the viscosity of the hydrogel is reduced drastically (Figure 2b). It reveals that the hydrogel exhibits shear-thinning behavior. A hysteresis (Figure 2c) can be observed in a cycle of the shear-rate sweep, which is known as a thixotropic loop, indicating that the hydrogel is thixotropic. The shear-thinning and thixotropic characteristics that are typical for pseudoplastic fluids<sup>[30]</sup> account for the easy shapeability or plasticity of the hybrid hydrogel. Additionally, the rheological behavior of the hydrogel is sensitive to temperature. When the temperature is higher than 65 °C,  $G'$  becomes higher than  $G''$ , corresponding to a harder hydrogel. The heat-induced hardening of the hydrogel might arise from more physical cross-links resulting from the increased mobility of PAA chains at high temperatures, and must be explored further.

Furthermore, dried in air, the ACC/PAA hydrogel can form free-standing, macroscopically continuous objects (flat or curved films, fibers), and this process is totally reversible (Figure 3a,b). The dry objects can recover the original hydrogel state without any loss of mechanical performance by letting them swell in water for one day. The drying–swelling process can be repeated many times. That means, our produced hydrogel can be easily recycled in this way, which has never been described for other mineral–polymer hybrid hydrogels. The dry objects are rigid with very smooth surface (SEM images in Figure S8). Taking the film for example, a nano-indentation measurement estimated its hardness and modulus to be  $1.0 \pm 0.07$  GPa and  $22.4 \pm 1.1$  GPa, respectively (Figure 3c), which are apparently much higher than its analogous biomineral, shrimp shell (hardness,  $0.172 \pm 0.023$  MPa; modulus,  $1.87 \pm 0.41$  GPa),<sup>[17]</sup> as well as conven-

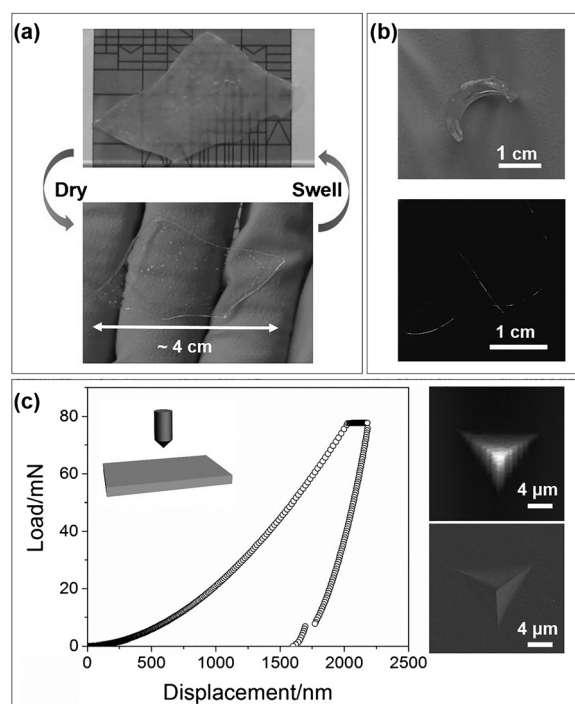


**Figure 3.** a) Drying an ACC/PAA hydrogel film results in a free-standing continuous transparent film, which can recover the hydrogel state after swelling in water, indicating this material is reversible. b) Other forms of the dried ACC/PAA hybrid such as curved films or fibers. c) Left: Loading–unloading nano-indentation curve for the ACC/PAA hybrid film. Right: the corresponding survey scanning and SEM images of the microstructure after indentation measurement.

tional plastics (e.g., for PMMA, hardness, 0.187 MPa; modulus, 3.83 GPa).<sup>[31]</sup> Such a good mechanical performance of the ACC/PAA hybrid material is really unexpected, especially considering that the ACC weight ratio is not high (47 wt %). We speculate that this performance is due to the formation of a densified nanocomposite structure during water evaporation by the slow self-adhesion of very small ACC nanoparticles in the hydrogel resulting in a defect-free bulk material. Indeed, judging from the survey scanning and SEM images (Figure 3c), the microstructure after indentation is also very smooth without cracks, indicating the film's good toughness. In contrary, when the chain length of PAA is short ( $M_w \approx 2000$  g mL<sup>−1</sup>), the resulting ACC/PAA hybrid film is fragile and discontinuous without the support of substrates,<sup>[18]</sup> and cannot be redispersed or swollen in water once dried (Figure S9).

Colorimetric materials are highly attractive for sensing, imaging, and display applications.<sup>[32]</sup> Therein, conjugated polydiacetylene (PDA) has been intensively investigated exhibiting an intense chromatic switch, typically from blue to red, in response to various external stimuli, such as temperature.<sup>[33]</sup> For instance, 10,12-pentacosadiynoic acid (PCDA, chemical structure in Figure S10) undergoes spontaneous molecular assembly in water to yield PCDA vesicles (transparent) that can be polymerized by UV irradiation (PDA vesicles, blue). Upon heating, an irreversible color change from blue to red occurs as a result of the disruption of



the planar conjugated structure.<sup>[34]</sup> We tested the ability of our ACC/PAA hydrogel and film as a matrix for colorimetric materials. Transparent ACC/PAA/PCDA hybrid films were fabricated by incorporating PCDA vesicles into the ACC/PAA hydrogel. As expected, the hybrid films (flat or curved) reproduce all the color changes of PDA vesicles, which are reflected by UV/Vis spectra (Figure 4). Their corresponding

hydrogel may be potentially applied as a new environmentally friendly and sustainable plastic material or “mineral plastics”.

### Experimental Section

**Preparation of ACC/PAA supramolecular hydrogel:** In a typical procedure, 0.1M Na<sub>2</sub>CO<sub>3</sub> was slowly injected into a vigorously stirred solution of 0.1M CaCl<sub>2</sub> and 0.1M PAA ( $M_w \approx 100\,000\text{ g mol}^{-1}$ , Aldrich). A white sticky precipitate gradually formed around the stirring bar with a turbid solution containing non-gelling fractions. After stirring for another hour, the turbid solution was discarded, and the hydrogel was washed with deionized water several times until the washing solution was clear.

To include dye molecules into the hydrogel, 0.08M rhodamine B or methylene blue was mixed with 0.1M Na<sub>2</sub>CO<sub>3</sub> before injecting into the solution of CaCl<sub>2</sub> and PAA.

For hydrogels of ACC/PAA 0.08 and ACC/PAA 0.2, only the concentration of PAA was adjusted to 0.08M and 0.2M, respectively.

**Preparation of free-standing ACC/PAA hybrid objects:** The hydrogel was shaped into films on flat glass plates or curved substrates, and left drying in air. After water removal, rigid transparent films can be obtained, which can be easily removed from the substrates. ACC/PAA hybrid microfibers were prepared by stretching the hydrogel or pulling from the bulk hydrogel with tweezers.

**Preparation of PCDA vesicles:** 2 mL of PCDA (Aldrich) in DMSO was slowly injected into 50 mL of deionized water at 80°C to yield a total monomer concentration of 1 mM. The resulting suspension was ultrasonicated for 30 min at ca. 80°C. Then the solution was filtered to remove lipid aggregates and kept at 4°C overnight before use.

**Preparation of ACC/PAA/PCDA supramolecular hydrogel:** For preparation, a mixed solution of 0.1M Na<sub>2</sub>CO<sub>3</sub> and 0.2 mM PCDA vesicles was slowly injected into a stock solution of 0.1M CaCl<sub>2</sub> and 0.1M PAA ( $M_w \approx 100\,000\text{ g mol}^{-1}$ ) with vigorous stirring. The resulting hydrogel or dry films were polymerized by 254 nm UV light for 5 min.

**Preparation of chemically cross-linked poly(*N,N*-dimethylacrylamide) hydrogel:** For the control experiment, poly(*N,N*-dimethylacrylamide) hydrogel was prepared by heating a mixed solution of *N,N*-dimethylacrylamide (33 wt %), *N,N*-methylene bis(acrylamide) (0.2 wt %), ammonium persulfate (0.3 wt %) at 60°C for 4 h. The obtained hydrogel was dyed by immersing in the aqueous solution of rhodamine B or methylene blue ( $10^{-3}\text{ M}$ ) for 3 h.

See characterization details in the Supporting Information.

### Acknowledgments

We gratefully acknowledge the financial support from the Alexander von Humboldt Foundation. This work was also supported by the facilities in the Nanostructure Laboratory of the University of Konstanz. S.H.Y. thanks funding support from National Science Foundation of China (Grants 21431006, 21521001). S.T.S. thanks Marina Krumova for TEM imaging, Dingding Hu in Fudan University for rheological measurements.

**Keywords:** amorphous calcium carbonate · bio-inspired synthesis · organic–inorganic hybrid composites · plasticity · supramolecular hydrogels

**How to cite:** *Angew. Chem. Int. Ed.* **2016**, 55, 11765–11769  
*Angew. Chem.* **2016**, 128, 11939–11943

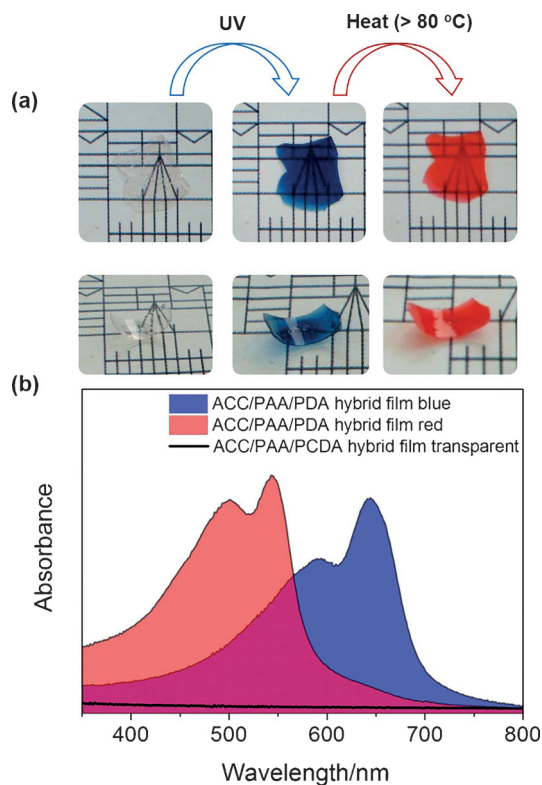


**Figure 4.** a) Color changes of ACC/PAA/PCDA hybrid films upon UV irradiation and heating. b) UV/Vis absorption profiles of the ACC/PAA/PCDA hybrid film and the blue and red films of ACC/PAA/PDA hybrid.

hydrogels exhibit similar good stretchability (Figure S11). This indicates that the ACC/PAA hybrid hydrogel and its rigid films can be very good matrices for thermochromic materials. Interestingly, the color change of the ACC/PAA/PDA hybrid film (blue to red) resembles that in the cooking process of blue shrimps (Figure S12).

In conclusion, inspired by PILP, we synthesized an ACC-based supramolecular hydrogel by simply mixing CaCl<sub>2</sub>, Na<sub>2</sub>CO<sub>3</sub>, and PAA. This hydrogel is shown to be shapeable, stretchable, self-healable, and reversible with shear-thinning and thixotropic properties. Reversible drying of the hydrogel under vapor-pressure control results in rigid, transparent, and continuous objects, exhibiting superior mechanical performance compared to its analogous biomineral (shrimp shell) and conventional plastics. Finally, thermochromic PDA vesicles can be introduced to the ACC/PAA hydrogel and hybrid film matrices, which show reproducible color changes upon UV irradiation and heat. In consideration of increasing environmental concerns arising from petroleum-based production of conventional plastics, our synthesized ACC-based

- [1] F. C. Meldrum, H. Cölfen, *Chem. Rev.* **2008**, *108*, 4332–4432.
- [2] M. A. Meyers, J. McKittrick, P.-Y. Chen, *Science* **2013**, *339*, 773–779.
- [3] U. G. K. Wegst, H. Bai, E. Saiz, A. P. Tomsia, R. O. Ritchie, *Nat. Mater.* **2015**, *14*, 23–36.
- [4] A.-W. Xu, Y. Ma, H. Cölfen, *J. Mater. Chem.* **2007**, *17*, 415–449.
- [5] N. Sommerdijk, H. Cölfen, *MRS Bull.* **2010**, *35*, 116–121.
- [6] F. Nudelman, N. A. J. M. Sommerdijk, *Angew. Chem. Int. Ed.* **2012**, *51*, 6582–6596; *Angew. Chem.* **2012**, *124*, 6686–6700.
- [7] P. M. Dove, J. De Yoreo, S. Weiner, *Biomaterialization*, Mineralogical Society of America, Washington, **2003**.
- [8] S. Weiner, I. Sagi, L. Addadi, *Science* **2005**, *309*, 1027–1028.
- [9] Y. Politi, T. Arad, E. Klein, S. Weiner, L. Addadi, *Science* **2004**, *306*, 1161–1164.
- [10] B.-A. Gotliv, N. Kessler, J. L. Sumerel, D. E. Morse, N. Tuross, L. Addadi, S. Weiner, *ChemBioChem* **2005**, *6*, 304–314.
- [11] L. Dai, E. P. Douglas, L. B. Gower, *J. Non-Cryst. Solids* **2008**, *354*, 1845–1854.
- [12] L. A. Gower, D. A. Tirrell, *J. Cryst. Growth* **1998**, *191*, 153–160.
- [13] L. B. Gower, *Chem. Rev.* **2008**, *108*, 4551–4627.
- [14] S. J. Homeijer, R. A. Barrett, L. B. Gower, *Cryst. Growth Des.* **2010**, *10*, 1040–1052.
- [15] A. Gal, W. Habraken, D. Gur, P. Fratzl, S. Weiner, L. Addadi, *Angew. Chem. Int. Ed.* **2013**, *52*, 4867–4870; *Angew. Chem.* **2013**, *125*, 4967–4970.
- [16] A. Mikkelsen, S. B. Engelsen, H. C. B. Hansen, O. Larsen, L. H. Skibsted, *J. Cryst. Growth* **1997**, *177*, 125–134.
- [17] T. Saito, Y. Oaki, T. Nishimura, A. Isogai, T. Kato, *Mater. Horiz.* **2014**, *1*, 321–325.
- [18] Y. Oaki, S. Kajiyama, T. Nishimura, H. Imai, T. Kato, *Adv. Mater.* **2008**, *20*, 3633–3637.
- [19] D. Gebauer, V. Oliynyk, M. Salajkova, J. Sort, Q. Zhou, L. Bergström, G. Salazar-Alvarez, *Nanoscale* **2011**, *3*, 3563–3566.
- [20] T. Nissinen, M. Li, S. A. Davis, S. Mann, *CrystEngComm* **2014**, *16*, 3843–3847.
- [21] E. Asenath-Smith, H. Li, E. C. Keene, Z. W. Seh, L. A. Estroff, *Adv. Funct. Mater.* **2012**, *22*, 2891–2914.
- [22] M. Kuang, D. Wang, M. Gao, J. Hartmann, H. Möhwald, *Chem. Mater.* **2005**, *17*, 656–660.
- [23] Z. A. C. Schnepp, R. Gonzalez-McQuire, S. Mann, *Adv. Mater.* **2006**, *18*, 1869–1872.
- [24] A. K. Gaharwar, S. A. Dammu, J. M. Canter, C.-J. Wu, G. Schmidt, *Biomacromolecules* **2011**, *12*, 1641–1650.
- [25] M. Helminger, B. Wu, T. Kollmann, D. Benke, D. Schwahn, V. Pipich, D. Faivre, D. Zahn, H. Cölfen, *Adv. Funct. Mater.* **2014**, *24*, 3187–3196.
- [26] Y. Xia, Y. Gu, X. Zhou, H. Xu, X. Zhao, M. Yaseen, J. R. Lu, *Biomacromolecules* **2012**, *13*, 2299–2308.
- [27] S. Kajiyama, T. Nishimura, T. Sakamoto, T. Kato, *Small* **2014**, *10*, 1634–1641.
- [28] X.-Z. Zhang, X.-D. Xu, S.-X. Cheng, R.-X. Zhuo, *Soft Matter* **2008**, *4*, 385–391.
- [29] L. Bromberg, M. Temchenko, V. Alakhov, T. A. Hatton, *Int. J. Pharm.* **2004**, *282*, 45–60.
- [30] K. Baezly, *Rheometry. Industrial Applications*, Research Studies Press, London, **1980**.
- [31] A.-Y. Jee, M. Lee, *Polym. Test.* **2010**, *29*, 95–99.
- [32] A. Seeboth, D. Löttsch, R. Ruhmann, O. Muehling, *Chem. Rev.* **2014**, *114*, 3037–3068.
- [33] D. J. Ahn, J.-M. Kim, *Acc. Chem. Res.* **2008**, *41*, 805–816.
- [34] O. Yarimaga, J. Jaworski, B. Yoon, J.-M. Kim, *Chem. Commun.* **2012**, *48*, 2469–2485.

Received: March 22, 2016

Published online: July 22, 2016